THE VIBRATION REDUCTION ANALYSIS OF A ROTATING MECHANISM DECK SYSTEM

Y.-R. Wang * **T.-H. Chen** **

Department of Aerospace Engineering
Tamkang University
Tamsui, Taiwan 25137, R.O.C.

ABSTRACT

In this paper, an optimized position of a mass-spring-damper vibration absorber is proposed for a rotating mechanism device (such as optical disk drive or rotary-wing and deck coupled system). A nonlinear 3-D theoretical model for a deck is established by Lagrange's equation. A 2-bladed rotor and deck (foundation) coupled aeroelastic system with vibration reduction device is presented and studied as well. The analytical solution is obtained by the Multiple-scales method for the case of no vibration absorber. The numerical results in time and frequency domain and with/no absorber are acquired. This research provides a theoretical background for the preliminary vibration reduction design for industries. It is found that the existing disk drives vibration can be reduced by simply adding the absorber at the end corner isolator of the deck, but without changing the main configurations. This will not only save costs but also increase testing efficiency, achieving the most cost-effective vibration reduction result.

Keywords : Vibration absorber, Rotating Fundation, Rotary-wing Blade.

1. INTRODUCTION

Vibration reduction of an optical disk drive or any of the rotating device deck such as rotary-wing coupled plate system by using a vibration absorber is presented in this paper. The traditional vibration reduction mechanism applied in normal optical disk is using the vibration isolator (also called damping washer) consisting of a resilient member (stiffness) and an energy dissipater (damping). Once the system of the disk drive is set, it is difficult to change the configuration, and so, the vibration reduction is limited for further modification. Furthermore, for the mini-scaled or micro-scaled unmanned rotary-wing aircraft, it is practically difficult to overcome the rotor shaft vibration by only the servo control. In this paper, a new vibration reduction device concept is presented for the optical disk drive or the mini-scaled unmanned rotary-wing aircraft.

For vibration-reduction, the development of all kinds of new dampers has allowed most kinds of vibration problems to be kept to a minimum. Developments in materials science have also resulted in various kinds of compound dampers in vibration-reduction solutions. In a published report on using damper attachments to moderate structural vibrations, Nakra [1] mentioned that compound structures made from metal and polymers can achieve the dampening effect while retaining strength and hardness. This has led to their use in a variety of machinery related industries such as aerospace, marine engineering, electronics and optical structures. For the optical disc drive, past vibration-reduction design focused on modifying the mass of the absorber so it achieved better vibration-reduction [2]. This however meant that different systems required different absorbers. A custom absorber must be built for each type of optical drive, significantly increasing costs. S. Tada *et al.* [3,4] examined the correlation between path tracking error and directional vibrations along the principal axis to study the frequencies of vibration sources on the main spindle. At the same time they also looked at how axial vibration affected overall system performance. Additionally, Chung *et al.* [5-7] proposed motion analyses for the free vibration of a spinning platter, platter vibration for non-linear angular acceleration and how automatic balancers reduce optical drive vibration. The above studies all analyzed the vibration of the entire optical drive system, but Jin Wook Heo *et al.* [8] proposed the concept of using a single vibration absorber to reduce the vibration and noise in existing optical drives. However, the optimal position has not been studied in their research. To improve the rotational mechanism (such as for optical drives) vibration and do so in an economic manner, this study sought to discover if simply changing the absorber position could achieve vibration reduction in the rotational mechanism without changing the absorber material or modifying the main structure of the mechanism.

* Associate Professor ** Graduate student

The basic model of this study uses four degrees of freedom (1 translation moving of a deck (Z_D), 2 rotation of a deck (θ_X, θ_Y) and 1 translation displacement of the absorber (Z_A) then derives the equations of motion of the deck-absorber coupled system using the Lagrange's equation. The θ_X and θ_Y are considered nonlinearly to allow large motions. The frequency domain response of deck amplitudes and the time domain phase plots of deck vibration velocities and displacements are studied. The numerical results are compared with the analytic solution to ensure its accuracy; from there, changes in the absorber position were observed to achieve vibration reduction. This study can be used in the vibration- reduction mechanism design of all rotation mechanisms such as hard disks, micro-scaled swahplate-less helicopters [9], and small rotor masts. This study is divided into two major parts. The first is the vibration- reduction analysis for standard optical drives or hard disks in order assess the effectiveness of the appliqué absorber. The second part is the vibration-reduction for an integrated system comprising a 2-bladed small main rotor and its foundation. This will hopefully open up new possibilities for appliqué absorbers.

2. THE EQUATIONS OF MOTION

See Fig. 1 for this deck's associated coordinates and definitions. M is the mass of the planar vibration deck. It is treated as a rigid body where m is the point mass of the absorber on which the deck is mounted. The point of origin for this system is the center of the deck, where C and d are the viscous damping coefficients; K and k are the Spring Constants; I_x and I_y are in the X and Y direction Moments of Inertia; X_i and Y_i (i = 1 ~ 4) represent the direction at X_i and Y_i as well as the distance from the point of origin; X_T and Y_T represent the distance to the point of incidence; X_A and Y_A represent the relative position between the absorber and the point of origin. With horizontal translation displacements in the X and Y direction not taken into account with rotation displacements in the Z direction, then Z_D is the deck displacing in the Z direction, Z_A is the displacement of the absorber in the Z direction towards the axis, while θ_x and θ_y is the plane's rotational angle in the X and Y direction and considered as geometrical non-linearity. Next, we considered a rotor mechanism with a set of two blades as shown in Fig. 2. If the blade's hinge with the mast is connected using a torsional spring, then the free body diagram for one single blade is as shown in Fig. 3. If the mast and vibration reduction deck are all rigid bodies, meaning that the lift generated by the rotor creates displacement in the Z direction that directly affects the deck, then the displacement caused by Z_D and the blade lift is considered no relative motion in this part. If the flapping angle (β) is an acute angle, then the kinetic energy T from the two blades is

$$T = 2\left[\frac{1}{2}I_B\Omega^2\beta^2+\frac{1}{2}I_B\dot{\beta}^2+\frac{1}{2}M_B\dot{Z}_D^2+\frac{1}{2}M_B(x_T\dot{\theta}_y)^2+\frac{1}{2}M_B(y_T\dot{\theta}_x)^2 - M_B x_T\dot{Z}_D\dot{\theta}_y+M_B y_T\dot{Z}_D\dot{\theta}_x-M_B x_T y_T\dot{\theta}_x\dot{\theta}_y\right]. \quad (1)$$

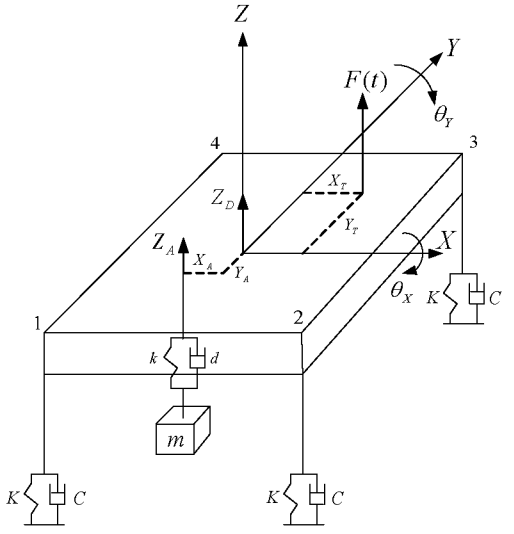

Fig. 1 Configuration of the deck and absorber

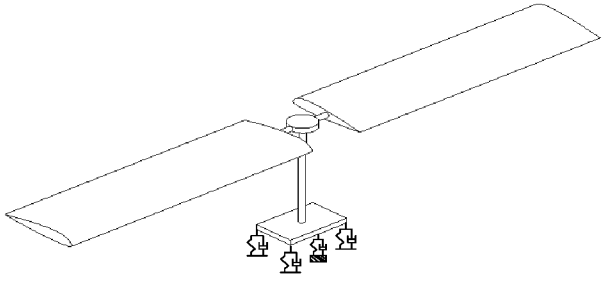

Fig. 2 Configuration of the rotor-deck coupled system

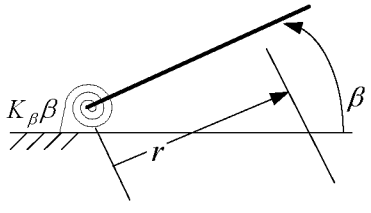

Fig. 3 Configuration of a single rotor blade

Here $I_B = \int_0^R r^2 dm_B$, M_B and R represent the blades' moment of inertia, mass and length while Ω is the rotor's speed of rotation. The potential energy V produced by the two blades is then

$$V = 2\left[\frac{1}{2}K_\beta\beta^2\right]. \quad (2)$$

Of these, K_β is the mast's torsional spring coefficient, while the work (W_{Lift}) done by the lift from the two blades is

$$W_{Lift} = 2\left\{\frac{1}{2}\rho ac\Omega^2\int_0^R\left[r^3\left(\theta-\frac{v_i+(\dot{Z}_D-x_T\dot{\theta}_y+y_T\dot{\theta}_x)+r\dot{\beta}}{\Omega r}\right)\right]dr\right\}. \quad (3)$$

where θ is the pitch angle of the blade, c is the chord of the blades and we set the induced flow as $v_i = 0.3R\Omega$. Once the two blades are coupled to the deck, we can then use the Lagrange's equation to derive the collective blade mode equation as

$$I_B\ddot{\beta}_C + \frac{1}{6}\rho acR^3\Omega\,(\dot{Z}_D - X_T\dot{\theta}_Y + Y_T\dot{\theta}_X) + \frac{1}{8}\rho acR^4\Omega\dot{\beta}_C + I_B\,\Omega^2\beta_C + k_B\,\beta_C = \frac{1}{8}\rho acR^4\Omega^2\theta - 0.05\rho acR^4\Omega^2\,. \tag{4}$$

Here β_C represents the flapping angle of the collective blade mode. While the differential blade mode equation for β is

$$I_B\ddot{\beta}_D + \frac{1}{8}\rho acR^4\Omega\dot{\beta}_D + (I_B\Omega^2 + k_B)\,\beta_D = 0\,. \tag{5}$$

Here β_D represents the flapping angle of the differential blade mode.

After the two blades are coupled to the deck, the kinetic energy and potential energy of the two blades as well as the kinetic energy and potential energy of the deck are combined, so the equation of motion for four degrees of freedom of the deck are:

Z_D equation of motion,

$$\begin{aligned}&(M+2M_B)\ddot{Z}_D + 2M_B\,Y_T\,\ddot{\theta}_X - 2M_B\,X_T\,\ddot{\theta}_Y\\ &+\left(4C + d + \frac{1}{2}\rho acR^2\Omega\right)\dot{Z}_D - d\dot{Z}_A\\ &+\left[\left(\sum_{i=1\sim4} Y_i\right)C + Y_A\,d + \frac{1}{2}\rho acR^2\Omega Y_T\right]\dot{\theta}_X\\ &-\left[\left(\sum_{i=1\sim4} X_i\right)C + X_A\,d + \frac{1}{2}\rho acR^2\Omega X_T\right]\dot{\theta}_Y\\ &+\frac{1}{3}\rho acR^3\Omega\,(\dot{\beta}_C + \dot{\beta}_D) + (4K+k)\,Z_D - kZ_A\\ &+\left[\left(\sum_{i=1\sim4} Y_i\right)K + Y_A\,k\right]\left(\theta_X + \frac{1}{3}{\theta_X}^3\right)\\ &-\left[\left(\sum_{i=1\sim4} X_i\right)K + X_A\,k\right]\left(\theta_Y + \frac{1}{3}{\theta_Y}^3\right)\\ &= \frac{1}{3}\rho acR^3\Omega^2\theta - \frac{0.3}{2}\rho acR^3\Omega^2\,,\end{aligned} \tag{6}$$

Z_A equation of motion,

$$m\ddot{Z}_A - d\dot{Z}_D + d\dot{Z}_A - (Y_A\,d)\,\dot{\theta}_X + (X_A\,d)\,\dot{\theta}_Y - kZ_D + kZ_A - (Y_A\,k)\left(\theta_X + \frac{1}{3}\theta_X^3\right) + (X_A\,k)\left(\theta_Y + \frac{1}{3}\theta_Y^3\right) = 0\,. \tag{7}$$

To simplify the problem so it meets the conditions for the Duffing equation, we disregarded the cross multiplication of the coupled terms within the equation — that is, all the cross-multiplying items between Z_D, Z_A, θ_X, and θ_Y were removed, so the equation for θ_X can be simplified to

$$\begin{aligned}&2M_B\,Y_T\,\ddot{Z}_D + (I_X + 2M_BY_T^2)\,\ddot{\theta}_X - 2M_B\,X_T\,Y_T\,\ddot{\theta}_Y\\ &+\left[\left(\sum_{i=1\sim4} Y_i\right)C + Y_A\,d + \frac{1}{2}\rho acR^2\Omega Y_T\right]\dot{Z}_D - (Y_A\,d)\dot{Z}_A\\ &+\left[\left(\sum_{i=1\sim4} Y_i^2\right)C + Y_A^2 d + \frac{1}{2}\rho acR^2\Omega Y_T^2\right]\dot{\theta}_X\\ &-\left[\left(\sum_{i=1\sim4} X_i\,Y_i\right)C + X_A\,Y_A d + \frac{1}{2}\rho acR^2\Omega X_T\,Y_T\right]\dot{\theta}_Y\\ &+\frac{1}{3}\rho acR^3\Omega Y_T(\dot{\beta}_C + \dot{\beta}_D) + \left[\left(\sum_{i=1\sim4} Y_i\right)K + Y_A\,k\right]\\ &Z_D - (Y_A\,k)\,Z_A + \left[\left(\sum_{i=1\sim4} Y_i^2\right)K + Y_A^2 k\right]\left(\theta_X + \frac{4}{3}\theta_X^3\right)\\ &-\left[\left(\sum_{i=1\sim4} X_i\,Y_i\right)K + X_A\,Y_A\,k\right]\left(\theta_Y + \frac{1}{3}{\theta_Y}^3\right)\\ &= \frac{1}{3}\rho acR^3\Omega^2\theta Y_T - \frac{0.3}{2}\rho acR^3\Omega^2 Y_T\,.\end{aligned} \tag{8}$$

By the same principle then the equation for θ_Y can be simplified to:

$$\begin{aligned}&-2M_BX_T\ddot{Z}_D - 2M_BX_TY_T\ddot{\theta}_X + (I_Y + 2M_B\,X_T^2)\,\ddot{\theta}_Y\\ &-\left[\left(\sum_{i=1\sim4} X_i\right)C + X_A\,d + \frac{1}{2}\rho acR^2\Omega X_T\right]\\ &\dot{Z}_D + (X_A\,d)\,\dot{Z}_A - \left[\left(\sum_{i=1\sim4} X_i\,Y_i\right)C + X_A\,Y_A\,d + \frac{1}{2}\rho acR^2\Omega X_T\,Y_T\right]\dot{\theta}_X\\ &+\left[\left(\sum_{i=1\sim4} X_i^2\right)C + X_A^2 d + \frac{1}{2}\rho acR^2\Omega X_T^2\right]\dot{\theta}_Y\\ &-\frac{1}{3}\rho acR^3\Omega X_T(\dot{\beta}_C + \dot{\beta}_D) - \left[\left(\sum_{i=1\sim4} X_i\right)K + X_A\,k\right]Z_D\\ &+(X_A\,k)Z_A - \left[\left(\sum_{i=1\sim4} X_i\,Y_i\right)K + X_A\,Y_A\,k\right]\left(\theta_X + \frac{1}{3}\theta_X^3\right)\\ &+\left[\left(\sum_{i=1\sim4} X_i^2\right)K + X_A^2 k\right]\left(\theta_Y + \frac{4}{3}\theta_Y^3\right)\\ &-\frac{1}{3}\rho acR^3\Omega^2\theta X_T + \frac{0.3}{2}\rho acR^3\Omega^2 X_T\,.\end{aligned} \tag{9}$$

It is noted that if no rotor is coupled, the equations of motion for the deck can be reduced to a four degrees of freedom system from Eqs. (6) ~ (9). The Z_D direction can be expressed in the following manner:

$$M\ddot{Z}_D + (4C+d)\,\dot{Z}_D - d\dot{Z}_A + \left[\left(\sum_{i=1\sim4} Y_i\right)C + Y_A d\right]\dot{\theta}_X - \left[\left(\sum_{i=1\sim4} X_i\right)C + X_A d\right]\dot{\theta}_Y + (4K+k)\,Z_D - kZ_A + \left[\left(\sum_{i=1\sim4} Y_i\right)K + Y_A k\right]\left(\theta_X + \frac{1}{3}\theta_X^3\right) - \left[\left(\sum_{i=1\sim4} X_i\right)K + X_A k\right]\left(\theta_Y + \frac{1}{3}\theta_Y^3\right) F(t), \quad (10)$$

Z_A directional equation of motion can be written as:

$$m\ddot{Z}_A - d\dot{Z}_D + d\dot{Z}_A - (Y_A d)\,\dot{\theta}_X + (X_A d)\,\dot{\theta}_Y - kZ_D + kZ_A - (Y_A k)\left(\theta_X + \frac{1}{3}\theta_X^3\right) + (X_A k)\left(\theta_Y + \frac{1}{3}\theta_Y^3\right) = 0. \quad (11)$$

The equation of motion for the θ_X direction can be simplified to

$$I_X\ddot{\theta}_X + \left[\left(\sum_{i=1\sim4} Y_i\right)C + Y_A d\right]\dot{Z}_D - (Y_A d)\,\dot{Z}_A + \left[\left(\sum_{i=1\sim4} Y_i^2\right)C + Y_A^2 d\right]\dot{\theta}_X - \left[\left(\sum_{i=1\sim4} X_i Y_i\right)C + X_A Y_A d\right]\dot{\theta}_Y + \left[\left(\sum_{i=1\sim4} Y_i\right)K + Y_A k\right]Z_D - (Y_A k)\,Z_A + \left[\left(\sum_{i=1\sim4} Y_i^2\right)K + Y_A^2 k\right]\left(\theta_X + \frac{4}{3}\theta_X^3\right) - \left[\left(\sum_{i=1\sim4} X_i Y_i\right)K + X_A Y_A k\right]\left(\theta_Y + \frac{1}{3}\theta_Y^3\right) = F(t)Y_T. \quad (12)$$

Similarly, the equation of motion for the θ_Y direction can be simplified to

$$I_Y\ddot{\theta}_Y - \left[\left(\sum_{i=1\sim4} X_i\right)C + X_A d\right]\dot{Z}_D + (X_A d)\,\dot{Z}_A - \left[\left(\sum_{i=1\sim4} X_i Y_i\right)C + X_A Y_A d\right]\dot{\theta}_X + \left[\left(\sum_{i=1\sim4} X_i^2\right)C + X_A^2 d\right]\dot{\theta}_Y - \left[\left(\sum_{i=1\sim4} X_i\right)K + X_A k\right]Z_D + (X_A k)\,Z_A - \left[\left(\sum_{i=1\sim4} X_i Y_i\right)K + X_A Y_A k\right]\left(\theta_X + \frac{1}{3}\theta_X^3\right) + \left[\left(\sum_{i=1\sim4} X_i^2\right)K + X_A^2 k\right]\left(\theta_Y + \frac{4}{3}\theta_Y^3\right) = -F(t)X_T. \quad (13)$$

where $F(t)$ is the external load of this deck system.

At this point we have derived the equations of motion for the deck and the rotor-deck coupled model. We can use the 4th order Runge-Kutta method to solve this directly and find out the effect of the vibration absorber on this mechanism. For Eqs. (4) ~ (9) and (10) ~ (13) we ignored the θ_X and θ_Y terms with an order greater than 3 to meet the classical form of Dufing equation. Additionally, we also had $Z_D = Z_{DC}\cos\omega t + Z_{DS}\sin\omega t$, $Z_A = Z_{AC}\cos\omega t + Z_{AS}\sin\omega t$, $\theta_X = \theta_{XC}\cos\omega t + \theta_{XS}\sin\omega t$, $\theta_Y = \theta_{YC}\cos\omega t + \theta_{YS}\sin\omega t$, $\theta = \bar{\theta}\sin\omega t$, $\beta_C = \beta_{CC}\cos\omega t + \beta_{CS}\sin\omega t$, $\beta_D = \beta_{DC}\cos\omega t + \beta_{DS}\sin\omega t$, and $F(t) = \bar{F}\sin\omega t$. Each equation was then separated into a $\cos\omega t$ and $\sin\omega t$ harmonic where the amplitude in the Z_D direction was $\sqrt{Z_{DC}^2 + Z_{DS}^2}$, in the Z_A direction was $\sqrt{Z_{AC}^2 + Z_{AS}^2}$, in the θ_X direction was $\sqrt{\theta_{XC}^2 + \theta_{XS}^2}$, in the θ_Y direction was $\sqrt{\theta_{YC}^2 + \theta_{YS}^2}$, in the β_C direction was $\sqrt{\beta_{CC}^2 + \beta_{CS}^2}$ and in the β_D direction was $\sqrt{\beta_{DC}^2 + \beta_{CS}^2}$. By substituting in different ω, we can acquire the frequency response for each degree of freedom.

3. THE ANALYTIC STUDY OF THE NON-LINEAR MODEL

3.1 The Analytic Study of the Deck Model

In this section, we shall use the Multiple-scales method [10] to solve this non-linear equation of motion for the deck model in order to verify the correctness of the numerical results. Due to the complexity of this non-linear equation of motion, we have left out the effect of the vibration absorber to make the solution easier to derive. First the Z_A related items in Eqs. (10), (12) and (13) are deleted with the remaining coefficients substituted by A_i, B_i and C_i (where $i = 1 \sim 8$). Among these $\Xi = F(t)$ simplifies each expression making them easy to develop, so Eqs. (10), (12) and (13) can be re-written as

$$A_1\ddot{Z}_D + A_2\dot{Z}_D + A_3\dot{\theta}_X + A_4\dot{\theta}_Y + A_5 Z_D + A_6\left(\theta_X + \frac{1}{3}\theta_X^3\right) + A_7\left(\theta_Y + \frac{1}{3}\theta_Y^3\right) = A_8\Xi, \quad (14)$$

$$B_1\ddot{\theta}_X + B_2\dot{Z}_D + B_3\dot{\theta}_X + B_4\dot{\theta}_Y + B_5 Z_D + B_6\left(\theta_X + \frac{4}{3}\theta_X^3\right) + B_7\left(\theta_Y + \frac{1}{3}\theta_Y^3\right) = B_8\Xi, \quad (15)$$

$$C_1\ddot{\theta}_Y + C_2\dot{Z}_D + C_3\dot{\theta}_X + C_4\dot{\theta}_Y + C_5 Z_D + C_6\left(\theta_X + \frac{1}{3}\theta_X^3\right) + C_7\left(\theta_Y + \frac{4}{3}\theta_Y^3\right) = C_8\Xi. \quad (16)$$

where A_i, B_i and C_i are the coefficients in Eqs. (10), (12) and (13), respectively.

We assumed a parameter ε, and this ε is used to identify the time scale. By setting $T_0 = t$ (fast rate of change of time), and $T_1 = \varepsilon t$ (slow rate of change of time)

then we can make the following assumption about the form of the desired solution:

$$Z_D(t;\varepsilon) = Z_{D0}(T_0, T_1, T_2, \cdots) + \varepsilon Z_{D1}(T_0, T_1, T_2, \cdots), \quad (17)$$

$$\theta_X(t;\varepsilon) = \theta_{X0}(T_0, T_1, T_2, \cdots) + \varepsilon\theta_{X1}(T_0, T_1, T_2, \cdots), \quad (18)$$

$$\theta_Y(t;\varepsilon) = \theta_{Y0}(T_0, T_1, T_2, \cdots) + \varepsilon\theta_{Y1}(T_0, T_1, T_2, \cdots). \quad (19)$$

The differential for the time of each equation can thus be written as:

$$\frac{\partial}{\partial t} = \frac{\partial}{\partial T_0} + \varepsilon\frac{\partial}{\partial T_1} + \cdots, \quad \frac{\partial^2}{\partial t^2} = \frac{\partial^2}{\partial T_0^2} + 2\varepsilon\frac{\partial^2}{\partial T_0 \partial T_1} + \cdots. \quad (20)$$

Using the above assumption and ignoring the ε with an order over two, Eqs. (14) to (16) can then be written in the following manner:

$$\begin{aligned} &A_1\frac{\partial^2}{\partial T_0^2}Z_{D0} + \varepsilon A_1\frac{\partial^2}{\partial T_0^2}Z_{D1} + 2\varepsilon A_1\frac{\partial^2}{\partial T_0 \partial T_1}Z_{D0} + A_5 Z_{D0} \\ &+ \varepsilon A_5 Z_{D1} = -\varepsilon\left[A_2\frac{\partial}{\partial T_0}Z_{D0} + A_3\frac{\partial}{\partial T_0}\theta_{X0} + A_4\frac{\partial}{\partial T_0}\theta_{Y0}\right. \\ &\left. + A_6\left(\theta_{X0} + \frac{1}{3}\theta_{X0}^3\right) + A_7\left(\theta_{Y0} + \frac{1}{3}\theta_{Y0}^3\right) - A_8\Xi\right], \end{aligned} \quad (21)$$

$$\begin{aligned} &B_1\frac{\partial^2}{\partial T_0^2}\theta_{X0} + \varepsilon B_1\frac{\partial^2}{\partial T_0^2}\theta_{X1} + 2\varepsilon B_1\frac{\partial^2}{\partial T_0 \partial T_1}\theta_{X0} + B_6\theta_{X0} + \varepsilon B_6\theta_{X1} \\ &= -\varepsilon\left[B_2\frac{\partial}{\partial T_0}Z_{D0} + B_3\frac{\partial}{\partial T_0}\theta_{X0} + B_4\frac{\partial}{\partial T_0}\theta_{Y0}\right. \\ &\left. + B_5 Z_{D0} + \frac{4}{3}B_6\theta_{X0}^3 + B_7\left(\theta_{Y0} + \frac{1}{3}\theta_{Y0}^3\right) - B_8\Xi\right], \end{aligned} \quad (22)$$

$$\begin{aligned} &C_1\frac{\partial^2}{\partial T_0^2}\theta_{Y0} + \varepsilon C_1\frac{\partial^2}{\partial T_0^2}\theta_{Y1} + 2\varepsilon C_1\frac{\partial^2}{\partial T_0 \partial T_1}\theta_{Y0} + C_7\theta_{Y0} + \varepsilon C_7\theta_{Y1} \\ &= -\varepsilon\left[C_2\frac{\partial}{\partial T_0}Z_{D0} + C_3\frac{\partial}{\partial T_0}\theta_{X0} + C_4\frac{\partial}{\partial T_0}\theta_{Y0} + C_5 Z_{D0}\right. \\ &\left. + C_6\left(\theta_{X0} + \frac{1}{3}\theta_{X0}^3\right) + \frac{4}{3}C_7\theta_{Y0}^3 - C_8\Xi\right]. \end{aligned} \quad (23)$$

We then split Eqs. (21) ~ (23) into two parts ε^0 and ε^1. The solution for the ε^0 part then becomes the following:

$$Z_{D0} = a_1(T_1, T_2, \cdots)\cos\left[\sqrt{\frac{A_5}{A_1}}T_0 + b_1(T_1, T_2, \cdots)\right], \quad (24)$$

$$\theta_{X0} = a_2(T_1, T_2, \cdots)\cos\left[\sqrt{\frac{B_6}{B_1}}T_0 + b_2(T_1, T_2, \cdots)\right], \quad (25)$$

$$\theta_{Y0} = a_3(T_1, T_2, \cdots)\cos\left[\sqrt{\frac{C_7}{C_1}}T_0 + b_3(T_1, T_2, \cdots)\right]. \quad (26)$$

The solution for Z_{D1} can also be found using the following equation (the ε^1 part):

$$\begin{aligned} &\frac{\partial^2}{\partial T_0^2}Z_{D1} + \frac{A_5}{A_1}Z_{D1} \\ &= \left(2\sqrt{\frac{A_5}{A_1}}\frac{\partial a_1}{\partial T_1} + \frac{A_2}{A_1}\sqrt{\frac{A_5}{A_1}}a_1\right)\sin\left(\sqrt{\frac{A_5}{A_1}}T_0 + b_1\right) \\ &+ 2\sqrt{\frac{A_5}{A_1}}a_1\frac{\partial b_1}{\partial T_1}\cos\left(\sqrt{\frac{A_5}{A_1}}T_0 + b_1\right) \\ &- \frac{A_6}{A_1}\left(a_2 + \frac{a_2^3}{4}\right)\cos\left(\sqrt{\frac{B_6}{B_1}}T_0 + b_2\right) \\ &+ \frac{A_3}{A_1}\sqrt{\frac{B_6}{B_1}}a_2\sin\left(\sqrt{\frac{B_6}{B_1}}T_0 + b_2\right) \\ &- \frac{A_6}{A_1}\frac{a_2^3}{12}\cos\left(3\sqrt{\frac{B_6}{B_1}}T_0 + 3b_2\right) \\ &- \frac{A_7}{A_1}\left(a_3 + \frac{a_3^3}{4}\right)\cos\left(\sqrt{\frac{C_7}{C_1}}T_0 + b_3\right) \\ &+ \frac{A_4}{A_1}\sqrt{\frac{C_7}{C_1}}a_3\sin\left(\sqrt{\frac{C_7}{C_1}}T_0 + b_3\right) \\ &- \frac{A_7}{A_1}\frac{a_3^3}{12}\cos\left(3\sqrt{\frac{C_7}{C_1}}T_0 + 3b_3\right) \\ &+ \frac{A_8}{A_1}\Xi. \end{aligned} \quad (27)$$

From Eq. (27), we can see that the modal frequency of Z_{D1} is $\sqrt{A_5/A_1}$. To prevent the occurrence of resonance, all coefficients with a frequency of $\sqrt{A_5/A_1}$ on the right-hand-side of Eq. (27) must be vanished. Therefore the following two equations are zero,

$$2\sqrt{\frac{A_5}{A_1}}\frac{\partial a_1}{\partial T_1} + \frac{A_2}{A_1}\sqrt{\frac{A_5}{A_1}}a_1 = 0, \quad (28)$$

$$2\sqrt{\frac{A_5}{A_1}}a_1\frac{\partial b_1}{\partial T_1} = 0. \quad (29)$$

By the same principle, the equation θ_{X1} can be arranged as below:

$$\begin{aligned} &\frac{\partial^2}{\partial T_0^2}\theta_{X1} + \frac{B_6}{B_1}\theta_{X1} = \left(2\sqrt{\frac{B_6}{B_1}}\frac{\partial a_2}{\partial T_1} + \frac{B_3}{B_1}\sqrt{\frac{B_6}{B_1}}a_2\right)\sin\left(\sqrt{\frac{B_6}{B_1}}T_0 + b_2\right) \\ &+ \left(2\sqrt{\frac{B_6}{B_1}}a_2\frac{\partial b_2}{\partial T_1} - \frac{B_6}{B_1}a_2^3\right)\cos\left(\sqrt{\frac{B_6}{B_1}}T_0 + b_2\right) - \frac{B_5}{B_1}a_1\cos\left(\sqrt{\frac{A_5}{A_1}}T_0 + b_1\right) \\ &+ \frac{B_2}{B_1}\sqrt{\frac{A_5}{A_1}}a_1\sin\left(\sqrt{\frac{A_5}{A_1}}T_0 + b_1\right) - \frac{B_6}{B_1}\frac{a_2^3}{3}\cos\left(3\sqrt{\frac{B_6}{B_1}}T_0 + 3b_2\right) \\ &- \frac{B_7}{B_1}\left(a_3 + \frac{a_3^3}{4}\right)\cos\left(\sqrt{\frac{C_7}{C_1}}T_0 + b_3\right) + \frac{B_4}{B_1}\sqrt{\frac{C_7}{C_1}}a_3\sin\left(\sqrt{\frac{C_7}{C_1}}T_0 + b_3\right) \\ &- \frac{B_7}{B_1}\frac{a_3^3}{12}\cos\left(3\sqrt{\frac{C_7}{C_1}}T_0 + 3b_3\right) + \frac{B_8}{B_1}\Xi. \end{aligned} \quad (30)$$

With the two following conditions,

$$2\sqrt{\frac{B_6}{B_1}}\frac{\partial a_2}{\partial T_1}+\frac{B_3}{B_1}\sqrt{\frac{B_6}{B_1}}a_2=0\,, \tag{31}$$

$$2\sqrt{\frac{B_6}{B_1}}a_2\frac{\partial b_2}{\partial T_1}-\frac{B_6}{B_1}a_2^3=0\,. \tag{32}$$

By the same principle, the equation θ_{Y1} can be arranged as below:

$$\begin{aligned}\frac{\partial^2}{\partial T_0^2}\theta_{Y1}+\frac{C_7}{C_1}\theta_{Y1}&=\left(2\sqrt{\frac{C_7}{C_1}}\frac{\partial a_3}{\partial T_1}+\frac{C_4}{C_1}\sqrt{\frac{C_7}{C_1}}a_3\right)\sin\left(\sqrt{\frac{C_7}{C_1}}T_0+b_3\right)\\
&+\left(2\sqrt{\frac{C_7}{C_1}}a_3\frac{\partial b_3}{\partial T_1}-\frac{C_7}{C_1}a_3^3\right)\cos\left(\sqrt{\frac{C_7}{C_1}}T_0+b_3\right)-\frac{C_5}{C_1}a_1\cos\left(\sqrt{\frac{A_5}{A_1}}T_0+b_1\right)\\
&+\frac{C_2}{C_1}\sqrt{\frac{A_5}{A_1}}a_1\sin\left(\sqrt{\frac{A_5}{A_1}}T_0+b_1\right)-\frac{C_6}{C_1}\left(a_2+\frac{a_2^3}{4}\right)\cos\left(\sqrt{\frac{B_6}{B_1}}T_0+b_2\right)\\
&+\frac{C_3}{C_1}\sqrt{\frac{B_6}{B_1}}a_2\sin\left(\sqrt{\frac{B_6}{B_1}}T_0+b_2\right)-\frac{C_6}{C_1}\frac{a_2^3}{12}\cos\left(3\sqrt{\frac{B_6}{B_1}}T_0+3b_2\right)\\
&-\frac{C_7}{C_1}\frac{a_3^3}{3}\cos\left(3\sqrt{\frac{C_7}{C_1}}T_0+3b_3\right)+\frac{C_8}{C_1}\Xi\,.\end{aligned} \tag{33}$$

By the same principle, with the following condition:

$$\sqrt{\frac{C_7}{C_1}}\frac{\partial a_3}{\partial T_1}+\frac{C_4}{C_1}\sqrt{\frac{C_7}{C_1}}a_3=0\,, \tag{34}$$

$$2\sqrt{\frac{C_7}{C_1}}a_3\frac{\partial b_3}{\partial T_1}-\frac{C_7}{C_1}a_3^3=0\,. \tag{35}$$

By solving Eqs. (28), (29), (31), (32), (34) and (35) with initial conditions, we can get the solutions for Z_{D1}, θ_{X1}, and θ_{Y1} as:

$$\begin{aligned}Z_{D1}&=\frac{1}{\frac{A_5}{A_1}-\frac{B_6}{B_1}}\left[-\frac{A_6}{A_1}\left(a_2+\frac{a_2^3}{4}\right)\cos\left(\sqrt{\frac{B_6}{B_1}}T_0+b_2\right)\right.\\
&\left.=+\frac{A_3}{A_1}\sqrt{\frac{B_6}{B_1}}a_2\sin\left(\sqrt{\frac{B_6}{B_1}}T_0+b_2\right)\right]\\
&-\frac{1}{\frac{A_5}{A_1}-9\frac{B_6}{B_1}}\frac{A_6}{A_1}\frac{a_2^3}{12}\cos\left(3\sqrt{\frac{B_6}{B_1}}T_0+3b_2\right)\\
&+\frac{1}{\frac{A_5}{A_1}-\frac{C_7}{C_1}}\left[-\frac{A_7}{A_1}\left(a_3+\frac{a_3^3}{4}\right)\cos\left(\sqrt{\frac{C_7}{C_1}}T_0+b_3\right)\right.\\
&\left.+\frac{A_4}{A_1}\sqrt{\frac{C_7}{C_1}}a_3\sin\left(\sqrt{\frac{C_7}{C_1}}T_0+b_3\right)\right]\\
&-\frac{1}{\frac{A_5}{A_1}-9\frac{C_7}{C_1}}\frac{A_7}{A_1}\frac{a_3^3}{12}\cos\left(3\sqrt{\frac{C_7}{C_1}}T_0+3b_3\right)+\frac{A_8}{A_5-A_1\omega^2}\Xi\end{aligned} \tag{36}$$

$$\begin{aligned}\theta_{X1}&=\frac{1}{\frac{B_6}{B_1}-\frac{A_5}{A_1}}\left[-\frac{B_5}{B_1}a_1\cos\left(\sqrt{\frac{A_5}{A_1}}T_0+b_1\right)\right.\\
&\left.+\frac{B_2}{B_1}\sqrt{\frac{A_5}{A_1}}a_1\sin\left(\sqrt{\frac{A_5}{A_1}}T_0+b_1\right)\right]\\
&+\frac{a_2^3}{24}\cos\left(3\sqrt{\frac{B_6}{B_1}}T_0+3b_2\right)\\
&+\frac{1}{\frac{B_6}{B_1}-\frac{C_7}{C_1}}\left[-\frac{B_7}{B_1}\left(a_3+\frac{a_3^3}{4}\right)\cos\left(\sqrt{\frac{C_7}{C_1}}T_0+b_3\right)\right.\\
&\left.+\frac{B_4}{B_1}\sqrt{\frac{C_7}{C_1}}a_3\sin\left(\sqrt{\frac{C_7}{C_1}}T_0+b_3\right)\right]\\
&-\frac{1}{\frac{B_6}{B_1}-9\frac{C_7}{C_1}}\frac{B_7}{B_1}\frac{a_3^3}{12}\cos\left(3\sqrt{\frac{C_7}{C_1}}T_0+3b_3\right)\\
&+\frac{B_8}{B_6-B_1\omega^2}\Xi\end{aligned} \tag{37}$$

$$\begin{aligned}\theta_{Y1}&=\frac{1}{\frac{C_7}{C_1}-\frac{A_5}{A_1}}\left[-\frac{C_5}{C_1}a_1\cos\left(\sqrt{\frac{A_5}{A_1}}T_0+b_1\right)\right.\\
&\left.+\frac{C_2}{C_1}\sqrt{\frac{A_5}{A_1}}a_1\sin\left(\sqrt{\frac{A_5}{A_1}}T_0+b_1\right)\right]\\
&+\frac{1}{\frac{C_7}{C_1}-\frac{B_6}{B_1}}\left[-\frac{C_6}{C_1}\left(a_2+\frac{a_2^3}{4}\right)\cos\left(\sqrt{\frac{B_6}{B_1}}T_0+b_2\right)\right.\\
&\left.+\frac{C_3}{C_1}\sqrt{\frac{B_6}{B_1}}a_2\sin\left(\sqrt{\frac{B_6}{B_1}}T_0+b_2\right)\right]\\
&-\frac{1}{\frac{C_7}{C_1}-9\frac{B_6}{B_1}}\frac{C_6}{C_1}\frac{a_2^3}{12}\cos\left(3\sqrt{\frac{B_6}{B_1}}T_0+3b_2\right)\\
&+\frac{a_3^3}{24}\cos\left(3\sqrt{\frac{C_7}{C_1}}T_0+3b_3\right)+\frac{C_8}{C_7-C_1\omega^2}\Xi\,.\end{aligned} \tag{38}$$

The solutions for Z_D, θ_X and θ_Y can now be easily acquired. By differentiating the time for the solutions of Z_D, θ_X and θ_Y it is also possible to derive their individual velocity expressions though these are omitted here in the interest of brevity.

3.2 Analytic Study of the Rotor and Deck Coupled Equation

In order to verify the numerical results, the Multiple-scales method was used to find the analytic solution. As for the simple deck analysis previously conducted, we have omitted the effect of the vibration absorber to make getting an analytic solution easier. We removed the Z_A related items in Eqs. (6), (8) and (9) then the re-

maining coefficients were substituted using A_i, B_i and C_i (where $i = 1 \sim 12$). It is noted that the coefficients (A_i, B_i and C_i) are different from Eqs. (14) ~ (16), although we use the same variables for simplicity. The coefficients in Eq. (4) were replaced with D_j ($j = 1 \sim 6$) and for Eq. (5) the coefficients were substituted with E_k ($k = 1 \sim 3$). This simplified the expression making it easier to solve, so Eqs. (4), (5), (6), (8) and (9) can be rewritten as:

$$D_1 \ddot{\beta}_C + D_2(\dot{Z}_D - X_T \dot{\theta}_Y + Y_T \dot{\theta}_X) + D_3 \dot{\beta}_C + D_4 \beta_C = D_5 \theta + D_6 , \tag{39}$$

$$E_1 \ddot{\beta}_D + E_2 \dot{\beta}_D + E_3 \beta_D = 0 , \tag{40}$$

$$A_1 \ddot{Z}_D + A_2 \ddot{\theta}_X + A_3 \ddot{\theta}_Y + A_4 \dot{Z}_D + A_5 \dot{\theta}_X + A_6 \dot{\theta}_Y + A_7(\dot{\beta}_C + \dot{\beta}_D) + A_8 Z_D + A_9\left(\theta_X + \frac{1}{3}\theta_X^3\right) + A_{10}\left(\theta_Y + \frac{1}{3}\theta_Y^3\right) = A_{11}\theta + A_{12} , \tag{41}$$

$$B_1 \ddot{Z}_D + B_2 \ddot{\theta}_X + B_3 \ddot{\theta}_Y + B_4 \dot{Z}_D + B_5 \dot{\theta}_X + B_6 \dot{\theta}_Y + B_7(\dot{\beta}_C + \dot{\beta}_D) + B_8 Z_D + B_9\left(\theta_X + \frac{4}{3}\theta_X^3\right) + B_{10}\left(\theta_Y + \frac{1}{3}\theta_Y^3\right) = B_{11}\theta + B_{12} , \tag{42}$$

$$C_1 \ddot{Z}_D + C_2 \ddot{\theta}_X + C_3 \ddot{\theta}_Y + C_4 \dot{Z}_D + C_5 \dot{\theta}_X + C_6 \dot{\theta}_Y + C_7(\dot{\beta}_C + \dot{\beta}_D) + C_8 Z_D + C_9\left(\theta_X + \frac{1}{3}\theta_X^3\right) + C_{10}\left(\theta_Y + \frac{4}{3}\theta_Y^3\right) = C_{11}\theta + C_{12} . \tag{43}$$

As described above, we assume a parameter ε. This parameter ε is used to identify the time scale, with the assumption that

$$\beta_C(t;\varepsilon) = \beta_{C0}(T_0, T_1, T_2) + \varepsilon\beta_{C1}(T_0, T_1, T_2) , \tag{44}$$

$$\beta_D(t;\varepsilon) = \beta_{D0}(T_0, T_1, T_2) + \varepsilon\beta_{D1}(T_0, T_1, T_2) , \tag{45}$$

$$Z_D(t;\varepsilon) = Z_{D0}(T_0, T_1, T_2, \cdots) + \varepsilon Z_{D1}(T_0, T_1, T_2, \cdots) , \tag{46}$$

$$\theta_X(t;\varepsilon) = \theta_{X0}(T_0, T_1, T_2, \cdots) + \varepsilon\theta_{X1}(T_0, T_1, T_2, \cdots) , \tag{47}$$

$$\theta_Y(t;\varepsilon) = \theta_{Y0}(T_0, T_1, T_2, \cdots) + \varepsilon\theta_{Y1}(T_0, T_1, T_2, \cdots) . \tag{48}$$

It is noted that we omitte those ε with orders greater than 2, we can further sort these into two equations ε^0 and ε^1. By following the previous step the solution for ε^0 part is as written below:

$$\beta_{C0} = a_4(T_1, T_2, \cdots)\cos\left[\sqrt{\frac{D_4}{D_1}}T_0 + b_4(T_1, T_2, \cdots)\right], \tag{49}$$

$$\beta_{D0} = 0 , \tag{50}$$

$$Z_{D0} = a_1(T_1, T_2, \cdots)\cos\left[\sqrt{\frac{A_8}{A_1}}T_0 + b_1(T_1, T_2, \cdots)\right], \tag{51}$$

$$\theta_{X0} = a_2(T_1, T_2, \cdots)\cos\left[\sqrt{\frac{B_9}{B_2}}T_0 + b_2(T_1, T_2, \cdots)\right], \tag{52}$$

$$\theta_{Y0} = a_3(T_1, T_2, \cdots)\cos\left[\sqrt{\frac{C_{10}}{C_3}}T_0 + b_3(T_1, T_2, \cdots)\right]. \tag{53}$$

The explanation for the ε^1 part is then as follows:

$$\begin{aligned}\beta_{C1} = {} & \frac{1}{\frac{D_4}{D_1} - \frac{A_8}{A_1}}\frac{D_2}{D_1}\sqrt{\frac{A_8}{A_1}}a_1\sin\left(\sqrt{\frac{A_8}{A_1}}T_0 + b_1\right) \\ & + \frac{Y_T}{\frac{D_4}{D_1} - \frac{B_9}{B_2}}\frac{D_2}{D_1}\sqrt{\frac{B_9}{B_2}}a_2\sin\left(\sqrt{\frac{B_9}{B_2}}T_0 + b_2\right) \\ & - \frac{X_T}{\frac{D_4}{D_1} - \frac{C_{10}}{C_3}}\frac{D_2}{D_1}\sqrt{\frac{C_{10}}{C_3}}a_3\sin\left(\sqrt{\frac{C_{10}}{C_3}}T_0 + b_3\right) \\ & + \frac{D_5}{D_4 - D_1\omega^2}\theta + \frac{D_6}{D_4}\left[1 - \cos\left(\sqrt{\frac{D_4}{D_1}}T_0\right)\right],\end{aligned} \tag{54}$$

$$\beta_{D1} = 0 , \tag{55}$$

$$\begin{aligned}Z_{D1} = {} & \frac{1}{\frac{A_8}{A_1} - \frac{B_9}{B_2}}\left\{\left[\left(\frac{A_2}{A_1}\frac{B_9}{B_2} - \frac{A_9}{A_1}\right)a_2 - \frac{1}{4}\frac{A_9}{A_1}a_2^3\right]\cos\left(\sqrt{\frac{B_9}{B_2}}T_0 + b_2\right)\right. \\ & \left. + \frac{A_5}{A_1}\sqrt{\frac{B_9}{B_2}}a_2\sin\left(\sqrt{\frac{B_9}{B_2}}T_0 + b_2\right)\right\} \\ & - \frac{1}{\frac{A_8}{A_1} - 9\frac{B_9}{B_2}}\frac{A_9}{A_1}\frac{a_2^3}{12}\cos\left(3\sqrt{\frac{B_9}{B_2}}T_0 + 3b_2\right) \\ & + \frac{1}{\frac{A_8}{A_1} - \frac{C_{10}}{C_3}}\left\{\left[\left(\frac{A_3}{A_1}\frac{C_{10}}{C_3} - \frac{A_{10}}{A_1}\right)a_3 - \frac{1}{4}\frac{A_{10}}{A_1}a_3^3\right]\cos\left(\sqrt{\frac{C_{10}}{C_3}}T_0 + b_3\right)\right. \\ & \left. + \frac{A_6}{A_1}\sqrt{\frac{C_{10}}{C_3}}a_3\sin\left(\sqrt{\frac{C_{10}}{C_3}}T_0 + b_3\right)\right\} \\ & - \frac{1}{\frac{A_8}{A_1} - 9\frac{C_{10}}{C_3}}\frac{A_{10}}{A_1}\frac{a_3^3}{12}\cos\left(3\sqrt{\frac{C_{10}}{C_3}}T_0 + 3b_3\right) \\ & + \frac{1}{\frac{A_8}{A_1} - \frac{D_4}{D_1}}\frac{A_7}{A_1}\sqrt{\frac{D_4}{D_1}}a_4\sin\left(\sqrt{\frac{D_4}{D_1}}T_0 + b_4\right) \\ & + \frac{A_{11}}{A_8 - A_1\omega^2}\theta + \frac{A_{12}}{A_8}\left[1 - \cos\left(\sqrt{\frac{A_8}{A_1}}T_0\right)\right],\end{aligned} \tag{56}$$

$$\theta_{X1}=\frac{1}{\frac{B_9}{B_2}-\frac{A_8}{A_1}}\left[\left(\frac{B_1}{B_2}\frac{A_8}{A_1}-\frac{B_8}{B_2}\right)a_1\cos\left(\sqrt{\frac{A_8}{A_1}}T_0+b_1\right)\right.$$
$$\left.+\frac{B_4}{B_2}\sqrt{\frac{A_8}{A_1}}a_1\sin\left(\sqrt{\frac{A_8}{A_1}}T_0+b_1\right)\right]$$
$$+\frac{a_2^3}{24}\cos\left(3\sqrt{\frac{B_9}{B_2}}T_0+3b_2\right)$$
$$+\frac{1}{\frac{B_9}{B_2}-\frac{C_{10}}{C_3}}\left\{\left[\left(\frac{B_3}{B_2}\frac{C_{10}}{C_3}-\frac{B_{10}}{B_2}\right)a_3-\frac{1}{4}\frac{B_{10}}{B_2}a_3^3\right]\cos\left(\sqrt{\frac{C_{10}}{C_3}}T_0+b_3\right)\right.$$
$$\left.+\frac{B_6}{B_2}\sqrt{\frac{C_{10}}{C_3}}a_3\sin\left(\sqrt{\frac{C_{10}}{C_3}}T_0+b_3\right)\right\}$$
$$-\frac{1}{\frac{B_9}{B_2}-9\frac{C_{10}}{C_3}}\frac{B_{10}}{B_2}\frac{a_3^3}{12}\cos\left(3\sqrt{\frac{C_{10}}{C_3}}T_0+3b_3\right)$$
$$+\frac{1}{\frac{B_9}{B_2}-\frac{D_4}{D_1}}\frac{B_7}{B_2}\sqrt{\frac{D_4}{D_1}}a_4\sin\left(\sqrt{\frac{D_4}{D_1}}T_0+b_4\right)$$
$$+\frac{B_{11}}{B_9-B_2\omega^2}\theta+\frac{B_{12}}{B_9}\left[1-\cos\left(\sqrt{\frac{B_9}{B_2}}T_0\right)\right],\qquad(57)$$

$$\theta_{Y1}=\frac{1}{\frac{C_{10}}{C_3}-\frac{A_8}{A_1}}\left[\left(\frac{C_1}{C_3}\frac{A_8}{A_1}-\frac{C_8}{C_3}\right)a_1\cos\left(\sqrt{\frac{A_8}{A_1}}T_0+b_1\right)\right.$$
$$\left.+\frac{C_4}{C_3}\sqrt{\frac{A_8}{A_1}}a_1\sin\left(\sqrt{\frac{A_8}{A_1}}T_0+b_1\right)\right]$$
$$+\frac{1}{\frac{C_{10}}{C_3}-\frac{B_9}{B_2}}\left\{\left[\left(\frac{C_2}{C_3}\frac{B_9}{B_2}-\frac{C_9}{C_3}\right)a_2-\frac{1}{4}\frac{C_9}{C_3}a_2^3\right]\cos\left(\sqrt{\frac{B_9}{B_2}}T_0+b_2\right)\right.$$
$$\left.+\frac{C_5}{C_3}\sqrt{\frac{B_9}{B_2}}a_2\sin\left(\sqrt{\frac{B_9}{B_2}}T_0+b_2\right)\right\}$$
$$-\frac{1}{\frac{C_{10}}{C_3}-9\frac{B_9}{B_2}}\frac{C_9}{C_3}\frac{a_2^3}{12}\cos\left(3\sqrt{\frac{B_9}{B_2}}T_0+3b_2\right)$$
$$+\frac{a_3^3}{24}\cos\left(3\sqrt{\frac{C_{10}}{C_3}}T_0+3b_3\right)$$
$$+\frac{1}{\frac{C_{10}}{C_3}-\frac{D_4}{D_1}}\frac{C_7}{C_3}\sqrt{\frac{D_4}{D_1}}a_4\sin\left(\sqrt{\frac{D_4}{D_1}}T_0+b_4\right)$$
$$+\frac{C_{11}}{C_{10}-C_3\omega^2}\theta+\frac{C_{12}}{C_{10}}\left[1-\cos\left(\sqrt{\frac{C_{10}}{C_3}}T_0\right)\right].\qquad(58)$$

Its velocity can also be easily derived by differentiating the time.

4. RESULT AND DISCUSSION

4.1 Results from Vibration Reduction Mechanism for the Deck

In this paper, the equation of motion we derived is in the classic Duffing equation. The 4th order Runge-Kutta Method can be applied to solve Eqs. (10) ~ (13) simultaneously. The time dependent solution and the effects of the absorber can be obtained. The frequency response for each degree of freedom can be determined by dividing Eqs. (10) ~ (13) into cos and sin parts with a simple harmonic input. The required reference data are listed in Table 1.

The analytic solutions of the deck (without absorber for easily analytic methodology) acquired from last section provide us a base line check for the numerical results. This analysis also provides a theoretical background for the preliminary vibration research.

In this study, we first performed an analysis on a deck with no vibration absorber. The numerical method was applied to the deck equations of motion but no absorber presented. Its external force coordinate was (XT, YT = 45,106mm), and its deck isolator's spring constant was 4196kg/sec^2 with a smaller deck viscous damping coefficient of 0.25kg/sec to make observation of vibrations easier. By applying both the numerical method and analytic solutions to the equation of motion, the results agreed with each other very well. Figure 4 was the ZD degree of freedom' phase diagram from numerical analysis. Figure 5 was the same degree of freedom' phase plot from analytic solution. From the above diagrams, we found that when each degree of freedom converges they all vibrate in the same zone so the results from the two methods match. The results are therefore reliable.

In this study, our vibration-reduction analysis was focused on changing the position of the vibration absorber in order to see how different vibration absorber placements affected the vibration amplitude. The deck's X and Y axes were therefore partitioned into four parts by diagonals as shown in Fig. 6. Since the external load position was fixed and the four vibration isolators were located on the corners of the deck, we consequently put the absorber to make a large moment arm in order to counteract the vibrations. Based on this thought, the possible best positions of the absorber could be on the end corners of the deck. Moreover, the positions of the diagonals can also provide us more information regarding this system's vibration amplitudes. The vibration absorber was then placed along the diagonals at a distance of 1/4, 2/4, 3/4 and 4/4 from the point of origin, and the four situations observed to see what effects it had. With the 1st quadrant as an example, the 1/4 coordinates relative to the point of origin are (19, 29.25), the 2/4 coordinates relative to the point of origin are (38, 58.5), the 3/4 coordinates relative to the origin are (57, 87.75) and the 4/4 coordinates relative to the point of origin are (76, 117). The same also applies to the remaining 2nd (−, +), 3rd (−, −) and 4th (+, −) quadrants. The mass of the vibration absorber is approximately 2% and in fact if it has too much mass it

Table 1 Properties of the deck-absorber system

Deck mass (kg)		0.164
Absorber mass (kg)	m	0.00328
Deck damper Coeff. (kg/sec)	C	5.68
Absorber damper Coeff. (kg/sec)	d	11.36
Deck spring Const. (kg/sec^2)	K	4916
Absorber spring Const. (kg/sec^2)	k	446
Moment of Inertia (x-dir.) (kg·mm^2)	I_x	300
Moment of Inertia (y-dir.) (kg·mm^2)	I_y	80
External force coordinate (x-dir) mm	X_T	45
External force coordinate (y-dir) mm	Y_T	106
Coordinate of deck's 4 corners (X_1 mm)	X_1	–76
Coordinate of deck's 4 corners (X_2 mm)	X_2	76
Coordinate of deck's 4 Corners (X_3 mm)	X_3	76
Coordinate of deck's 4 Corners (X_4 mm)	X_4	–76
Coordinate of deck's 4 Corners (Y_1 mm)	Y_1	–117
Coordinate of deck's 4 Corners (Y_2 mm)	Y_2	–117
Coordinate of deck's 4 Corners (Y_3 mm)	Y_3	117
Coordinate of deck's 4 Corners (Y_4 mm)	Y_4	117

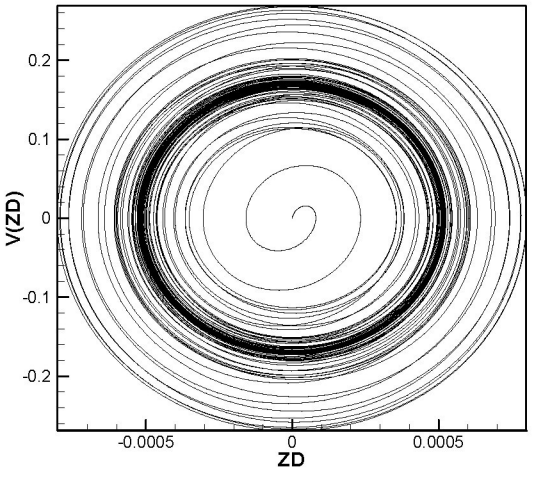

Fig. 4 Phase plot of Z_D (numerical method)

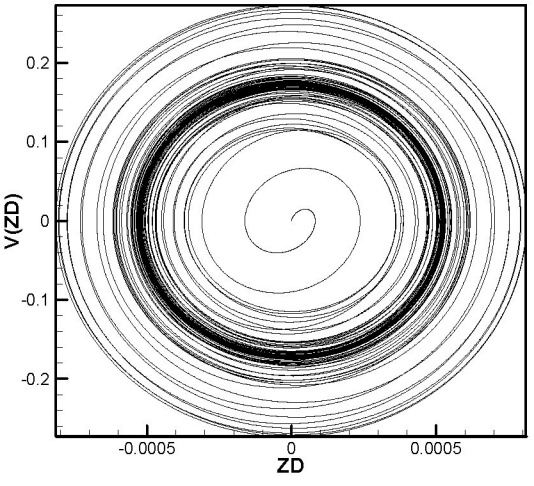

Fig. 5 Phase plot of Z_D (analytical method)

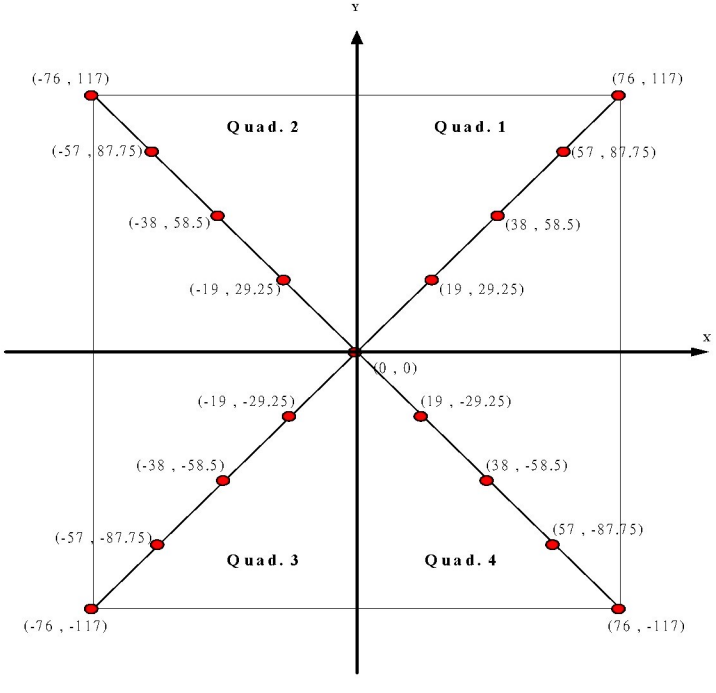

Fig. 6 Diagonal locations of the absorber

Table 2 The effect of absorber on $|Z_D|$

Absorber position (mm)	$\|Z_D\|_{max}$ (10^{-4}mm)			Resonant frequency (rad/sec)
	Frequency Response	Runge-Kutta Method	Linear Result	
$Xa = 0$, $Ya = 0$	1.3040799	1.3040795	1.2388758	329.0
$Xa = 57$, $Ya = 87.75$	1.3280159	1.3280159	1.2616151	329.0
$Xa = 76$, $Ya = 117$	1.3360969	1.3360965	1.2692920	329.0
$Xa = -57$, $Ya = 87.75$	1.3090641	1.30906454	1.2436109	329.0
$Xa = -76$, $Ya = 117$	1.3105442	1.3105443	1.2450170	329.0
$Xa = -57$, $Ya = -87.75$	1.2793457	1.2793455	1.2153785	328.0
$Xa = -76$, $Ya = -117$	1.2706181	1.2706182	1.2070872	328.0
$Xa = 57$, $Ya = -87.75$	1.2981096	1.2981093	1.2332039	329.0
$Xa = 76$, $Ya = -117$	1.2958012	1.2958010	1.2310111	329.0

Table 3 The effect of absorber on $|\theta_X|$

Absorber position (mm)	$\|\theta_X\|_{max}$ (10^{-10}rad)			Resonant frequency (rad/sec)
	Frequency Response	Runge-Kutta Method	Linear Result	
$Xa = 0$, $Ya = 0$	4.2988017	4.2978402	4.0838617	600.0
$Xa = 57$, $Ya = 87.75$	4.3291590	4.3291629	4.1127009	605.0
$Xa = 76$, $Ya = 117$	4.3886143	4.3886183	4.1691834	599.0
$Xa = -57$, $Ya = 87.75$	4.2198158	4.2166718	4.0088247	600.0
$Xa = -76$, $Ya = 117$	4.1954218	4.1954274	3.9856505	593.0
$Xa = -57$, $Ya = -87.75$	4.5304898	4.5304961	4.3039654	588.0
$Xa = -76$, $Ya = -117$	4.6670581	4.6670539	4.4337051	579.0
$Xa = 57$, $Ya = -87.75$	4.4239283	4.4239329	4.2027321	577.0
$Xa = 76$, $Ya = -117$	4.4797184	4.4797198	4.2557323	563.0

Table 4 The effect of absorber on $|\theta_Y|$

Absorber position (mm)	$\|\theta_Y\|_{max}$ (10^{-10}rad)			Resonant frequency (rad/sec)
	Frequency Response	Runge-Kutta Method	Linear Result	
$Xa = 0$, $Ya = 0$	3.9674291	3.9674285	3.7690577	273.0
$Xa = 57$, $Ya = 87.75$	4.1409996	4.1409680	3.9339494	295.0
$Xa = 76$, $Ya = 117$	4.2383206	4.2383215	4.0264047	298.0
$Xa = -57$, $Ya = 87.75$	4.1064484	4.1064499	3.9011260	413.0
$Xa = -76$, $Ya = 117$	4.1527278	4.1527232	3.9450913	413.0
$Xa = -57$, $Ya = -87.75$	4.2705710	4.2705688	4.0570427	456.0
$Xa = -76$, $Ya = -117$	4.4579537	4.4579508	4.2350561	491.0
$Xa = 57$, $Ya = -87.75$	4.0475447	4.0475436	3.8451674	283.0
$Xa = 76$, $Ya = -117$	4.0680393	4.0680379	3.8646374	283.0

conflicts with the principle of cost-effectiveness and keeping weight down. To simplify the problem, we therefore chose not to factor in the effect of change of its moment of inertia I_X and I_Y. We can use the largest amplitude found in the frequency response to find out its corresponding region for comparison. The primary goal of this study is to observe the effect on vibration-reduction from moving the vibration absorber. The Z_A degrees of freedom represent the vibration absorber's own vibration amplitude. We will not discuss this aspect here and only observe the three degrees of freedom for Z_D, θ_X and θ_Y. From the data in Tables 2 to 4, it can be projected that the effectiveness of the vibration absorber will vary in accordance with its distance from the origin and with changes in moment arm distance. The linear model results are included in the tables for comparison. It was found that for this deck if the absorber is moved to the furthest point of incidence (in this example, the corner of the 3rd quadrant) it can effectively suppress transverse vibrations though its ability to suppress vibrations in the rotational direction (θ_x, θ_y) is impaired. Both linear and nonlinear models discovered this effect. It is noted that the nonlinear model shows larger amplitudes than the linear model, we believe that the nonlinear terms still have contributions to this system (although are limited). However, for an optical disk or the micro devices, a tiny vibration may cause reading data errors or other unpredicted damages. Furthermore, when we examined Tables 2 to 4 closely it was found that the maximum transverse Z_D amplitude was much greater than the rotation amplitudes (θ_x, θ_y), so the actual effect should still be based on Z_D. The vibration in this direction may need more attention on the preliminary design of this system.

4.2 Results from Vibration-Reduction Mechanism of Coupled Rotor and Deck

The reference rotor data required in this study is listed in Table 5 and the pitch angle selected for the rotor blade was $10° \approx 0.1745$rad. First an analytical approach is taken to define a deck structure with no absorber; its data are shown in Table 1. As the rotor blade transmits far more force, a higher viscous damping coefficient of 45kg/sec was selected first so the graph can be more easily observed. Using the numerical method (Runge-Kutta method) with its equation of motion, the phase diagram at the time domain when its Z_D degrees of freedom achieve convergence was acquired and was plotted with the convergent result from analytical method shown in Fig. 7. We found that when convergence was achieved, both vibrated in the same zone so the results correlate. The results of this study are therefore reliable.

Next, we study the cases of the absorber presented. Equations (4) to (9) are considered both in Runge-Kutta method or frequency response. By using the frequency response analysis perspective to validate this mode, we tested the vibration absorber at the position (19, 29.25) to see the amplitude relationship between Z_D, Z_A, θ_X, and θ_Y as well as how it relates to the frequency. First we observed that when the vibration absorber was located (19, 29.25), the displacement of Z_D can be seen in Fig. 8, when $\omega = 9.3$Hz the amplitude is around 1.2747. The maximum displacement from time dependent result is 1.2715 so there's an error of 0.3%. Next, from Fig. 9 we can see that when $\omega = 9.3$Hz, the vibration amplitude of Z_A is 1.7533. Compared to the maximum displacement from time dependent of 1.7531, the error is approximately 0.01%. The vibration amplitude of θ_X can be seen in Fig. 10. When $\omega = 9.3$Hz, the vibration amplitude is approximately 9.6197E−03. Compared to the maximum displacement from time dependent of 9.5953E−03, the error is approximately 0.3%. The vibration amplitude of θ_Y can be seen in Fig. 11. When $\omega = 9.3$Hz, the vibration amplitude is approximately 9.6661E−03. Compared to the maximum displacement from time dependent of 9.85940E−03, the error is approximately 2%. The results are proved to be reliable. During this we observed that when $\omega = 6.7$Hz, the four degrees of freedom in Z_D, Z_A, θ_X, and θ_Y decrease rapidly. This is because this frequency is the resonant frequency of the flapping angle so it causes rapid fluctuations in the deck vibration amplitude. For a better view of this phenomenon, the magnified resonant area of Z_D plot (Fig. 8) is shown in Fig. 12. Consider an undamped and decoupled blade-flapping mode from Eq. (4), we can obtain the natural frequency of β_C mode.

Table 5 Properties of the rotor system

Mass of the rotor blade (kg)	M_B	1.29345
Moment of inertia of the blade (kg·mm^2)	I_B	323362.5
Torsional spring Constant (N·mm/rad)	K_β	166352000
Blade length (span) (mm)	R	500
Blade chord length (mm)	c	30.5
Rotor speed (rad/sec)	Ω	35.63
Blade lift slope	a	6
Air density (kg·mm^3)	ρ	1.22674×10^{-9}

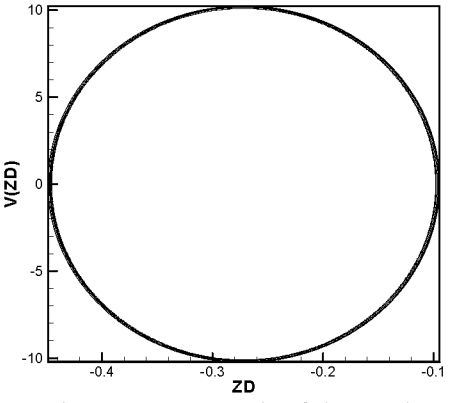

Fig. 7 The convergent cycle of the Z_D phase plot (numerical and analytical method)

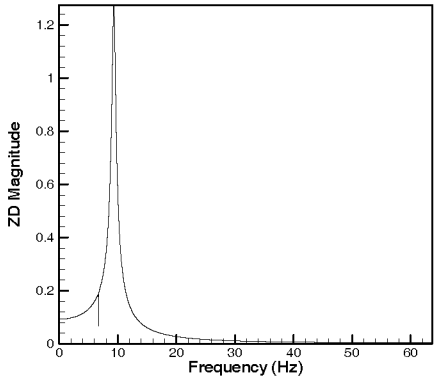

Fig. 8 The | Z_D | frequency response (absorber location (19, 29.25))

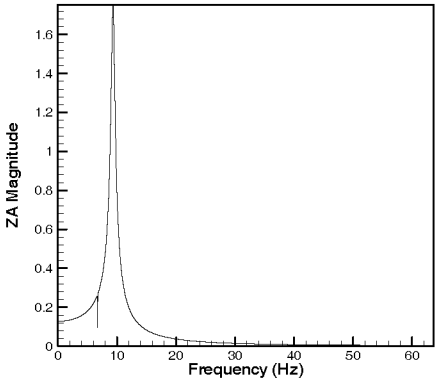

Fig. 9 The | Z_A | frequency response (absorber location (19, 29.25))

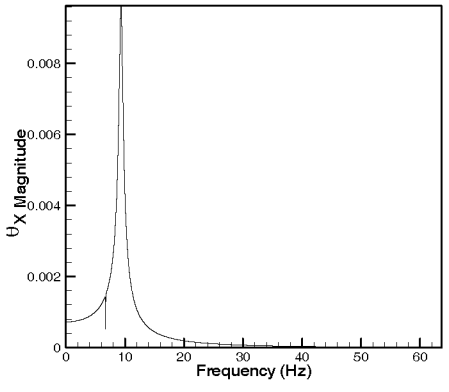

Fig. 10 The | θ_X | frequency response (absorber location (19, 29.25))

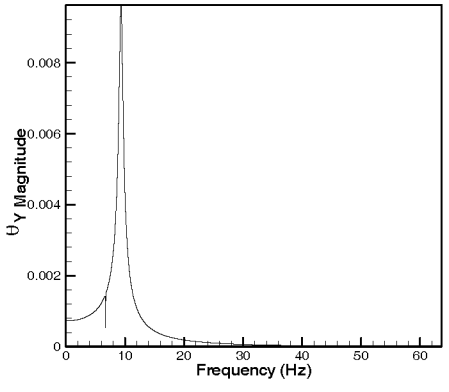

Fig. 11 The | θ_Y | frequency response (absorber location (19, 29.25))

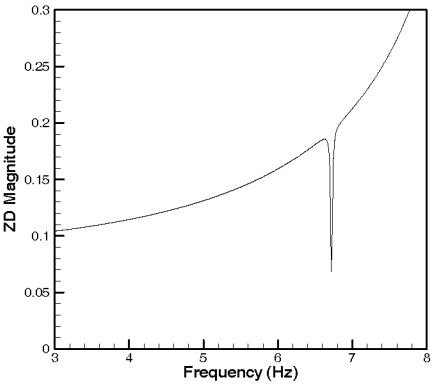

Fig. 12 A magnified resonant area from Fig. 8

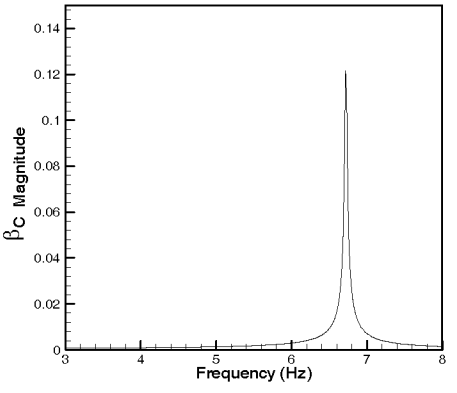

Fig. 13 The collective blade mode (β_C) frequency response

Using the data from Table 5, one can acquire the natural frequency as 6.71Hz for β_C. The plot of the collective flap mode is shown in Fig. 13. It shows that the spike appears at 6.71Hz, and this becomes a significant result in the system and should be concerned in the future design.

In this study, we coupled the rotor blade with the deck with the external force that had been applied to the deck replaced by the lift generated from the rotor blades. The vibration reduction analysis was still based on the absorber's position however to see how the positioning of the absorber affects the magnitude of vibration amplitude. See Fig. 6 for the absorber's positioning. The main goal of this study is to observe the effect of changing the absorber's positioning on vibration reduction for the deck. Only the three degrees of freedom θ_X, θ_Y and Z_D were therefore observed. From the data in Tables 6 to 8, it can be projected that the effectiveness of the vibration absorber will vary in accordance with its distance from the origin and with changes in moment arm distance. The linear model results are again included in the tables for comparison. It was found that for this coupled rotor and deck system, just like for the deck only system, if the vibration absorber is moved to the furthest point of incidence (in this example, the corner of the 3rd quadrant) it can effectively suppress transverse vibrations, though its ability to suppress vibrations in the rotational direction is impaired. However, the transverse Z_D amplitude was much greater than the rotation amplitudes (θ_x, θ_y), so the actual effect should still be based on Z_D.

Table 6 The effect of absorber on $|Z_D|$ (rotor-deck system)

Absorber position (mm)	$\|Z_D\|_{max}$ (mm)			Resonant frequency (rad/sec)
	Frequency Response	Runge-Kutta Method	Linear Result	
$Xa = 0$, $Ya = 0$	1.274638	1.271582	1.195469	58.6
$Xa = 57$, $Ya = 87.75$	1.274766	1.271133	1.195579	58.6
$Xa = 76$, $Ya = 117$	1.274629	1.270692	1.195446	58.6
$Xa = -57$, $Ya = 87.75$	1.274717	1.271608	1.195541	58.6
$Xa = -76$, $Ya = 117$	1.274738	1.271576	1.195560	58.6
$Xa = -57$, $Ya = -87.75$	1.273992	1.271059	1.194866	58.6
$Xa = -76$, $Ya = -117$	1.273691	1.270663	1.194583	58.6
$Xa = 57$, $Ya = -87.75$	1.274537	1.271569	1.195375	58.6
$Xa = 76$, $Ya = -117$	1.274499	1.271540	1.195340	58.6

Table 7 The effect of absorber on $|\theta_X|$ (rotor-deck system)

Absorber position (mm)	$\|\theta_X\|_{max}$ (10^{-6}rad)			Resonant frequency (rad/sec)
	Frequency Response	Runge-Kutta Method	Linear Result	
$Xa = 0$, $Ya = 0$	9.6188141	9.5954277	9.0222117	58.6
$Xa = 57$, $Ya = 87.75$	9.6234130	9.5956493	9.0264529	58.6
$Xa = 76$, $Ya = 117$	9.6258838	9.5958328	9.0287365	58.6
$Xa = -57$, $Ya = 87.75$	9.6238907	9.6000591	9.0269623	58.6
$Xa = -76$, $Ya = 117$	9.6260244	9.6018482	9.0289610	58.6
$Xa = -57$, $Ya = -87.75$	9.6206153	9.5982356	9.0239234	58.6
$Xa = -76$, $Ya = -117$	9.6228654	9.5998188	9.0260291	58.6
$Xa = 57$, $Ya = -87.75$	9.6157324	9.5928814	9.0193292	58.6
$Xa = 76$, $Ya = -117$	9.6151512	9.5923441	9.0187872	58.6

Table 8 The effect of absorber on $|\theta_Y|$ (rotor-deck system)

Absorber position (mm)	$\|\theta_Y\|_{max}$ (10^{-6}rad)			Resonant frequency (rad/sec)
	Frequency Response	Runge-Kutta Method	Linear Result	
$Xa = 0$, $Ya = 0$	9.6641043	9.8601254	9.0646995	58.6
$Xa = 57$, $Ya = 87.75$	9.6739782	9.8600173	9.0738889	58.6
$Xa = 76$, $Ya = 117$	9.6794348	9.8612597	9.0789720	58.6
$Xa = -57$, $Ya = 87.75$	9.6544763	9.8491516	9.0556564	58.6
$Xa = -76$, $Ya = 117$	9.6504772	9.8444801	9.0519004	58.6
$Xa = -57$, $Ya = -87.75$	9.6661532	9.8686833	9.0666441	58.6
$Xa = -76$, $Ya = -117$	9.6697146	9.8733651	9.0699820	58.6
$Xa = 57$, $Ya = -87.75$	9.6702259	9.8680016	9.0704514	58.6
$Xa = 76$, $Ya = -117$	9.6714962	9.8697571	9.0716453	58.6

5. CONCLUSIONS

This study successfully used several methods including the Runge-Kutta method, the frequency response, and the Multiple-scales method to prove the correctness of the non-linear equations for the motion constructed. It also successfully discovered the best vibration absorber positioning to minimize a rotating mechanism's deck vibration is to set it parallelly with the four corners' isolator of the deck, depending on the positioning of the external force. Additionally, this result's process and results are summarized as follow:

(1) Deck Only Structure

1. The four degrees of freedom Z_D, Z_A, and nonlinear θ_X and θ_Y are mutually dependent, and this study was able to successfully emulate this combination.
2. It was found that the maximum transverse Z_D amplitude was much greater than the rotation amplitudes (θ_x, θ_y), so the actual effect should still be based on Z_D. The vibration in this direction may need more attention on the preliminary design of this system.
3. The best position for the vibration absorber to minimize the vibration in the deck is at the end corner of the deck of the diagonal to the point of incidence.

(2) Coupled Rotor and Deck Structure

1. When the blade's pitch angle (θ) frequency is the resonant frequency of their flapping angle, the three degrees of freedom Z_D, θ_X and θ_Y fluctuate greatly.
2. The best position for the vibration absorber to minimize the coupled vibration system is at the end corner of the deck of the diagonal to the point of incidence.
3. This research has successfully proven that the vibration absorber's position can be changed to achieve the vibration reduction effect. It is therefore unnecessary to change the vibration absorber material or modify the greater part of the deck. To achieve vibration reduction, simply lock the vibration absorber to different locations. Although this can be predicted based on basic vibration theory, no other research works regarding this subject are presented. This study provides a theoretical background for the preliminary vibration reduction design for industries. This will not only save costs but also increase testing efficiency, achieving the most cost- effective vibration reduction result.

REFERENCES

1. Nakra, B. C., "Vibration Control with Viscoelastic Materials," *Shock and Vibration Digest,* 8, pp. 3–12 (1976).
2. Japan Patent, No. 2,951,943.
3. Tada, S., Yanbe, S., and Inoue, Y., "Study on Tracking Error of Magnet-Optical Disk Drive," *JSME* (in Japanese), August, pp. 2657–2663 (1994).
4. Tada, S., Yanbe, S., and Nakajima, K., "Axial Vibration of Optical Disk Spindle System," *JSME* (in Japanese), December, pp. 45–52 (1996).
5. Chung, J., Kang, N. C., and Lee, J. M., "A Study on Free Vibration of a Spinning Disk," *KSME International Journal*, 10, pp. 138–145 (1996).
6. Chung, J. and Oh, J.-E., and Yoo, H. H., "Nonlinear Vibration of a Flexible Spinning Disk with Angular Acceleration," *Journal of Sound and Vibration*, 232, pp. 375–391 (2000).
7. Chung, J. and Ro, D. S., "Dynamic Analysis of an Automatic Dynamic Balancer for Rotating Mechanisms," *Journal of Sound and Vibration*, 228, pp. 1035–1056 (1999).
8. Heo, J. W., Chung, J. T. and Park, J. M., "Vibration and Noise Reduction of an Optical Disk Drive by Using a Vibration Absorber," *Consumer Electronics*, IEEE Transactions, 48, pp. 874–878 (2002).
9. Nikhil, A. K. and Chopra, I., "Open-Loop Hover Testing of a Smart Rotor Model," *AIAA Journal*, 40, pp. 1495–1502 (2002).
10. Nayfeh, A. H., *Introduction to Perturbation Techniques*, Wiley-Interscience, New York (1981).

(Manuscript received April 1, 2007,
accepted for publication November 20, 2007.)